

## A DFT-D4 investigation of the complexation phenomenon between pentachlorophenol and $\beta$ -cyclodextrin

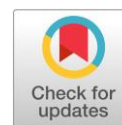
Zoubir Kabouche <sup>a</sup>, Youghourta Belhocine <sup>b</sup> \* , Tahar Benlecheb <sup>a</sup>,  
Ibtissem Meriem Assaba <sup>bc</sup>, Abdelkarim Litim <sup>a</sup>, Rabab Lalalou <sup>b</sup>,  
Asma Mechhoud <sup>b</sup>

**a:** Laboratory of Sensors, Instrumentations and Process (LCIP), University of Abbes Laghrour, Khenchela 40000, Algeria

**b:** Laboratory of catalysis, bioprocess and environment, Department of Process Engineering, Faculty of Technology, University of 20 August 1955, Skikda 21000, Algeria

**c:** LRPCSI-Laboratoire de Recherche sur la Physico-Chimie des Surfaces et Interfaces, University of 20 August 1955, Skikda 21000, Algeria

\* Corresponding author: [y.belhocine@univ-skikda.dz](mailto:y.belhocine@univ-skikda.dz)



This paper belongs to a Regular Issue.

### Abstract

Density functional theory (DFT) calculations based on the BLYP-D4 and PBEh-3c composite methods were performed for investigating the encapsulation mode of pentachlorophenol (PCP) inside the cavity of  $\beta$ -cyclodextrin ( $\beta$ -CD). Different quantum chemical parameters such as HOMO, LUMO, and HOMO–LUMO gap were calculated. Complexation energies were computed at the molecular level to provide insight into the inclusion of PCP inside the  $\beta$ -CD cavity. The Independent gradient model (IGM) approach was applied to characterize the non-covalent interactions that occurred during the complex (PCP@ $\beta$ -CD) formation. Two modes of inclusion were considered in this work (modes A and B). Calculated complexation energies as well as the changes in enthalpy, entropy, and free Gibbs energy exhibit negative values for both modes A and B, indicating a thermodynamically favorable process. Weak Van der Waals interactions and one strong intermolecular hydrogen bond act as the main driving forces behind the stabilization of the formed most stable complex. This study was carried out to explore the potential use of the  $\beta$ -CD as a host macrocycle for sensing and capturing pentachlorophenol.

### Keywords

$\beta$ -cyclodextrin  
pentachlorophenol  
inclusion complex  
non-covalent interactions  
environmental pollution

Received: 25.02.23

Revised: 15.04.23

Accepted: 21.04.23

Available online: 28.04.23

### Key findings

- The complexation process between  $\beta$ -cyclodextrin and pentachlorophenol is spontaneous, exothermic and enthalpy-driven.
- Pentachlorophenol is partially included in the  $\beta$ -cyclodextrin cavity.
- Stabilization of Pentachlorophenol@ $\beta$ -cyclodextrin complex is due to hydrogen bonding and Van der Waals interactions.
- The sensing potential of  $\beta$ -cyclodextrin towards pentachlorophenol could be used for environmental monitoring.

© 2023, the Authors. This article is published in open access under the terms and conditions of the Creative Commons Attribution (CC BY) license (<http://creativecommons.org/licenses/by/4.0/>).

## 1. Introduction

The host-guest chemistry has paved the way for the development of supramolecular nanoarchitectures [1] with practical applications such as molecular recognition, drug delivery and electrochemical biosensing [2–4]. Host–guest assemblies consist of guest molecules bound to the host molecules through non-covalent interactions (van der Waals forces, hydrogen bonding, hydrophobic effect,  $\pi$ – $\pi$  stacking interactions, etc.). Among the different classes of macrocyclic

systems, calixarenes [5], pillararenes [6], cucurbiturils [7], and, in particular, cyclodextrins [8–10] are the widely used host molecules in host-guest chemistry. The usefulness of these host molecules lies in their ability to enhance the solubility, stability and bioavailability of poorly water-soluble guests through the complexation process [11, 12].

Cyclodextrins (CDs) represent a family of cyclic oligosaccharides with unique properties that belong to the cage molecules family; they are usually used as host systems able to be complexed with a wide variety of guests. On the

other hand, CDs are inexpensive and eco-friendly, which makes them suitable for use in several industries [13]. CDs are considered as semi-natural products synthesized by simple enzymatic conversion of starch and containing six to twelve glucopyranose units [14–16]; they possess a hydrophilic peripheral surface and hydrophobic interior cavity with an overall truncated cone shape [17, 18].  $\alpha$ -,  $\beta$ -, and  $\gamma$ -cyclodextrins, composed, respectively, of six, seven, and eight glucopyranose units, represent the three main common cyclodextrins [19].

Pentachlorophenol (PCP) is an industrial prevalent wood preservative used since 1936, particularly, in utility poles and railway ties [20]. Its widespread use has caused environment pollution. Indeed, the PCP was listed among the 126 priority pollutants by the European Community as well as the United States Environmental Protection Agency (USEPA) [21] and was classified as a potentially carcinogenic compound by USEPA and International Agency for Research on Cancer (IARC) [22]. Its use has been, therefore, severely regulated in many countries since 1987, except for the preservation of wood that is limited to industrial uses [23]. Consequently, the biodegradation of this toxic substance has attracted growing interest among scientists and researchers with the aim of developing experimental methods for the removal of PCP.

An alternative method for the capture of PCP molecules through the supramolecular chemistry concept consists in the encapsulation of PCP by host macrocyclic systems such as cyclodextrins, cucurbiturils, calixarenes, etc. The complexation of guest molecules in the cavity of host systems, particularly,  $\beta$ -cyclodextrin, induces modifications in the physicochemical properties of the guests [24, 25].

Theoretical investigations of the host-guest interactions were the subject of several studies with the aim of understanding the complexation behavior at molecular level by determining the forces involved in the stabilization of guest molecules inside the cavities of the macrocyclic hosts. For this purpose, different quantum chemical methods ranging from semi-empirical ones such as AM1, PM3, PM6 and PM7 [26–28] to density functional theory based approaches [29–31] were employed.

In this paper, we performed a theoretical study based on the density functional theory (DFT) method, aiming at investigating the inclusion phenomenon between the  $\beta$ -cyclodextrin ( $\beta$ -CD) host system and the pentachlorophenol (PCP) guest molecule. The formation of a 1:1 stoichiometry complex was the subject of a previous experimental study [32], while the present work constitutes a complementary approach to rationalizing the inclusion phenomenon.

## 2. Computational procedure

ORCA code (version 4.2.1) [33, 34] was utilized to perform DFT calculations. The whole complexation process consists of full geometry optimization of the initial generated complexes formed between pentachlorophenol (PCP) and  $\beta$ -

cyclodextrin ( $\beta$ -CD) in vacuum using BLYP-D4 functional [35–39] associated with the def2-SVP basis set. A geometrical counterpoise correction scheme (gCP) [40] was applied to account for the basis set superposition error (BSSE). Based on the approach proposed by Liu and Guo [41], the center of PCP (guest) and  $\beta$ -CD (host) was set as the center of the coordinate system (0 Å). The guest molecule, PCP, was translated with a step of 1 Å from -8 to +8 Å along the Z-axis, resulting thus in two possible inclusion modes on the side of the wider rim of the  $\beta$ -CD, denoted A or B. These modes correspond to the inclusion orientation of the PCP through  $\beta$ -CD cavity by its terminal chloro group or its hydroxy group (OH), respectively, as represented in Figure 1 (a and b) using the visualization application Jmol [42]. For a more precise inspection of the lowest energy conformations, we explored and included more initial conformations in the vicinity of the most stable configurations. Thus, a step of 0.5 Å was considered for A and B modes along the Z-axis in the ranges [0–8 Å] and [2–8 Å], respectively. A total of 48 possible conformations were obtained and fully optimized in vacuum at BLYP-D4/def2-SVP-gCP level of theory, without any symmetry constraints.

The complexation energies were calculated using equation (1):

$$\Delta E_{\text{Complexation}} = E_{\text{Complex(PCP@}\beta\text{-CD)}} - (E_{\text{PCP}} + E_{\beta\text{-CD}}), \quad (1)$$

where  $\Delta E_{\text{Complexation}}$ ,  $E_{\text{ComplexPCP@}\beta\text{-CD}}$ ,  $E_{\text{PCP}}$ , and  $E_{\beta\text{-CD}}$  represent, respectively, the complexation energy, the optimized energies of the complex, the free PCP, and the free  $\beta$ -CD.

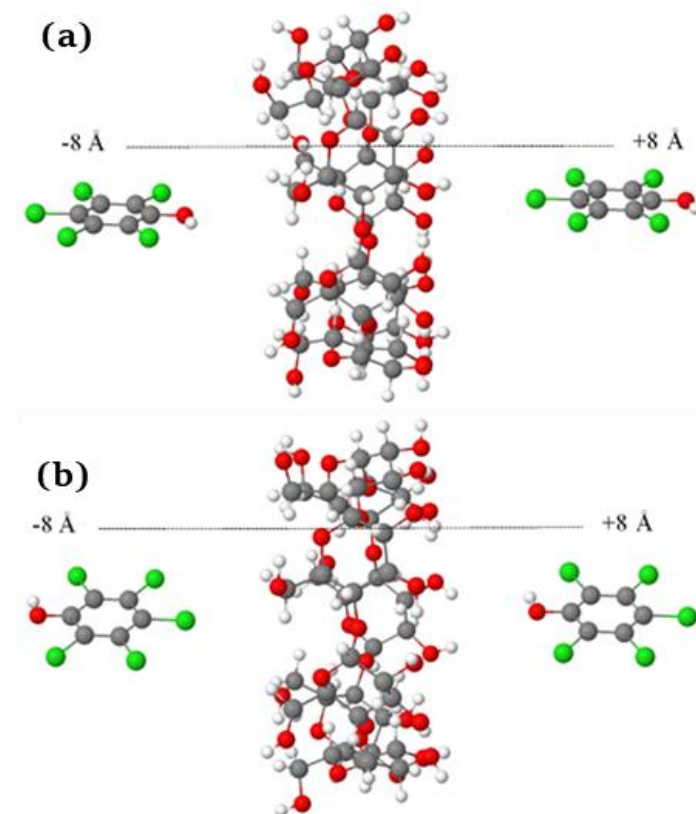


**Figure 1** Schematic illustration of the inclusion complexation conformations (Mode A) (a) and Mode B (b). Atomic color code: carbon (grey), hydrogen (white), oxygen (red), chlorine (green).

The most stable configurations correspond to the structures with the lowest complexation energies. The obtained most stable structures calculated at BLYP-D4/def2-SVP-gCP level of theory for A and B modes were subsequently reoptimized with the more accurate global hybrid PBEh-3c [43] functional in both vacuum and aqueous phase. Calculations in water solvent were performed with the SMD solvation model [44]. Then, the most stable geometry associated with the lowest energy structure was subjected to further analyses, such as non-covalent interactions (NCIs) characterization with independent gradient model based on the Hirshfeld partitioning scheme (IGMH) [45, 46] using Multwfn code [47] and VMD program for visualization [48].

### 3. Results and Discussion

#### 3.1. DFT-calculations of complexation energies

The most stable configuration corresponds to the lowest energy of all the optimized conformations calculated at DFT/BLYP-D4/def2-SVP-gcp level of theory. Figure 2 reports the values of the computed complexation energy for the A and B modes for each optimized conformation.

The energy profiles obtained for all configurations in both modes (A and B) exhibit negative complexation energy values, pointing out a thermodynamically favorable process. Full geometry optimization was followed by frequency calculations to verify that the obtained structures are true minima. Overall, the complexation energies are globally less negative for the A and B configurations located at the negative positions of Z-axis (from  $-8 \text{ \AA}$  to  $-1 \text{ \AA}$ ), whereas more negative values of the complexation energies are observed in the interval of positive values of z axis points.

The most stable configurations for A and B modes are located at  $Z = 7.5$  and  $6.5 \text{ \AA}$ , with the respective complexation energies of  $-121.39$  and  $-123.79 \text{ kJ/mol}$ . The re-optimization at PBEh-3c level yielded complexation energies of  $-69.00$  and  $-70.66 \text{ kJ/mol}$  in vacuum and  $-21.02$  and  $-29.53 \text{ kJ/mol}$  in water solvent for  $7.5 \text{ A}$  and  $6.5 \text{ B}$  configurations, respectively, with the complex PCP@ $\beta$ -CD of B mode being more stable than that of A mode.

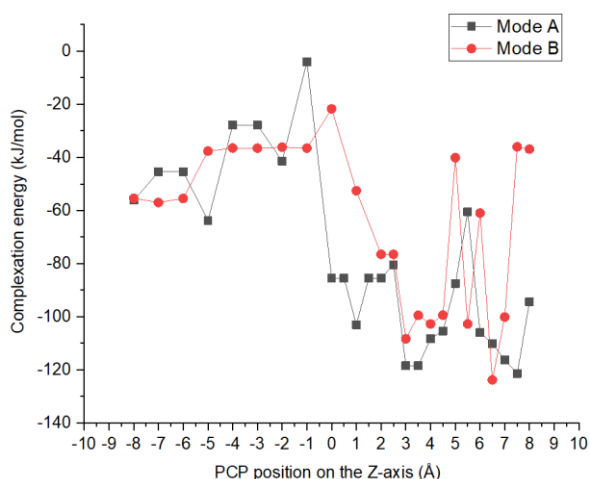


**Figure 2** Energy profile of the complexation between PCP and  $\beta$ -CD (A and B modes).

The complexation process is thermodynamically more favorable in vacuum than in the water solvent. The structural analysis of the most stable PCP@ $\beta$ -CD complex configuration (mode B at  $6.5 \text{ \AA}$ ) calculated with PBEh-3c in vacuum shows the partial pentachlorophenol encapsulation inside the  $\beta$ -CD cavity, as illustrated in Figure 3.

It is worth mentioning that the least stable structure located at  $Z = -1 \text{ \AA}$  for A mode with a complexation energy of  $-4.05 \text{ kJ/mol}$  corresponds structurally to the inclusion of the PCP into the  $\beta$ -CD cavity, as shown in Figure 4. Indeed, the  $\beta$ -CD cavity is not sufficiently large to encapsulate completely the PCP guest within; the total inclusion of PCP involves strong elongation and flattening of  $\beta$ -CD.

The obtained results suggest that the stability of the molecular association between PCP and  $\beta$ -CD is enhanced by the partial encapsulation of the PCP guest. The inclusion of PCP depends mainly on the cavity size of  $\beta$ -CD.

#### 3.2. Quantum electronic parameters

The energies of the frontier molecular orbitals (HOMO and LUMO), and the molecular HOMO-LUMO gap of the most stable inclusion complex were computed at DFT/PBEh-3c level in vacuum, and the obtained results are shown in Table 1.

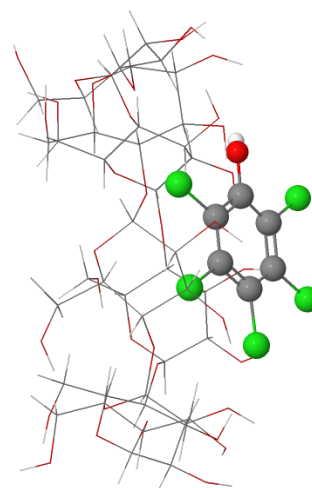


**Figure 3** Side view of the most stable configuration of the complex PCP@ $\beta$ -CD showing the partial encapsulation of PCP inside  $\beta$ -CD cavity.

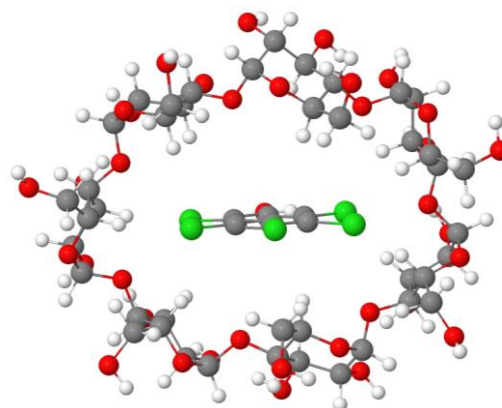


**Figure 4** Front view of the least stable configuration of the complex PCP@ $\beta$ -CD.

The HOMO–LUMO energy gap is reduced from 9.915 eV for the host molecule  $\beta$ -CD to 6.883 eV after complexation by a percentage variation of about 30.58%, indicating, thus, the potential use of  $\beta$ -CD as a host for PCP detection. The HOMO and LUMO of the most stable PCP@ $\beta$ -CD complex was visualized with IboView program [49, 50] and represented in Figure 5. Both HOMO and LUMO are almost entirely delocalized over the fused PCP molecule.

The HOMO–LUMO energy gap can be used as an indicator of kinetic stability. A large energy separation is associated with a low chemical reactivity and high kinetic stability. Upon the complexation, the decrease in the HOMO–LUMO gap of the PCP@ $\beta$ -CD complex (6.88 eV) in comparison with  $\beta$ -CD alone (9.92 eV) indicates that PCP@ $\beta$ -CD complex is more reactive and less stable than  $\beta$ -CD.

### 3.3. Characterization of the intermolecular non-covalent interactions

The IGMH analysis was performed to provide insights into the nature of the intermolecular non-covalent interactions involved in the stabilization of the PCP@ $\beta$ -CD complex. The IGMH plots are colored according to the occurring intermolecular interactions. Green and blue colors denote, respectively, weak Van der Waals and hydrogen-bond interactions. The IGMH isosurface of the most stable PCP@ $\beta$ -CD complex (Figure 6) was calculated using Multiwfn and visualized with the VMD program.

The topological analysis shows that green areas associated with Van der Waals interactions dominated the calculated isosurface; the presence of a one hydrogen bond is revealed by the blue disc, as represented in Figure 6, indicating that both weak Van der Waals interactions and the single intermolecular hydrogen bond act as attractive forces for the stabilization of PCP@ $\beta$ -CD complex.

### 3.4. Statistical thermodynamic calculations

The thermodynamic parameters were calculated at PBEh-3c level of theory in vacuum using frequency calculation analysis for the most stable configuration.

**Table 1** Frontier orbitals and HOMO–LUMO gap for  $\beta$ -CD, PCP, and PCP@ $\beta$ -CD system.

Parameters	$\beta$ -CD	PCP	PCP@ $\beta$ -CD
$E_{\text{HOMO}}$	-8.107	-7.841	-7.762
$E_{\text{LUMO}}$	1.808	-0.854	-0.879
$\Delta E_{\text{gap}}$	9.915	6.988	6.883

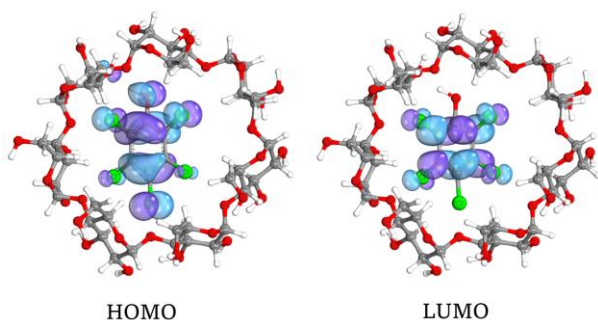


**Figure 5** HOMO and LUMO orbitals of PCP@ $\beta$ -CD complex.

The enthalpy, entropy, and Gibbs free energy changes [51, 52] of the complexation process of PCP with  $\beta$ -CD at standard temperature and pressure values (298.15 K and 1 atm) are reported in Table 2. The calculated  $\Delta G^\circ$  value is negative, showing that the complexation process is spontaneous. In addition, the negative values of enthalpy and entropy changes ( $\Delta H^\circ$  and  $\Delta S^\circ$ ) indicated that the process is enthalpy-controlled and exothermic in nature.

### 3.5. Natural orbital bond (NBO) analysis of intermolecular interactions

The NBO approach [53] provides useful insights for describing and determining the nature of the different donor-acceptor interactions that occur in the molecular systems. The NBO analysis was carried out on the relaxed geometry of the most stable complex at Mo6-2X/def2-TZVPP [54–56] level of theory in vacuum using Gaussian 09 program [57]. The structural analysis (Figure 7) shows the presence of one strong hydrogen bond having a stabilization energy of 139.03 kJ/mol, formed between hydrogen atom H (160) of terminal CHO group of  $\beta$ -CD as the donor and oxygen atom O (121) of the PCP as the acceptor with a short distance of 1.62 Å.

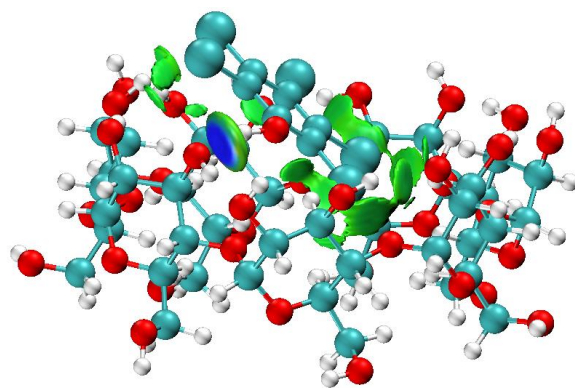


**Figure 6** The IGMH isosurface (isovalue 0.005 a.u.) of the PCP@ $\beta$ -CD complex.

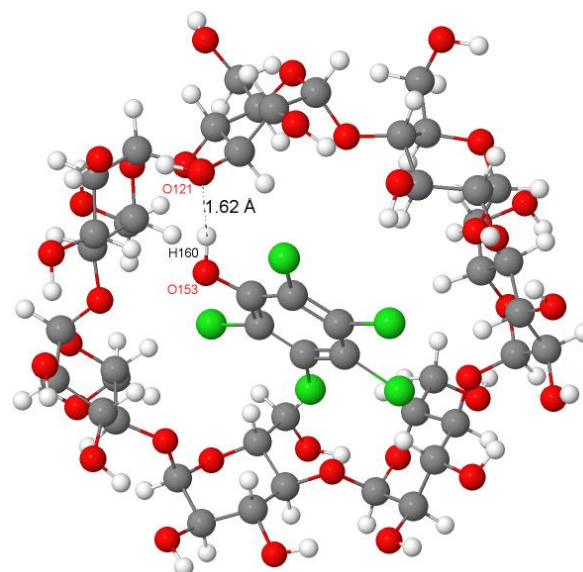


**Figure 7** The significant intermolecular hydrogen bonds for the PCP@ $\beta$ -CD complex.

**Table 2** Energetic and thermodynamic parameters of the complexation process calculated at PBEh-3c levels of theory in vacuum.

Thermodynamic Parameters	Energetic values
$\Delta H^\circ$ (kJ/mol)	-66.85
$\Delta G^\circ$ (kJ/mol)	-1.25
$\Delta S^\circ$ (kJ/mol)	-65.61

## 4. Limitations

Performing DFT calculations using several functionals and several basis sets is useful for comparison purposes; however, the high computational and time cost of such calculations are the limiting factors.

## 5. Conclusion

The energetic and electronic properties of the complexation process between pentachlorophenol (PCP) and  $\beta$ -cyclodextrin were computationally studied using DFT approach. The main conclusions of the present investigation can be stated as follows:

- Calculated thermodynamic parameters exhibit negative enthalpy, entropy and Gibbs energy changes, indicating that the complexation process is spontaneous, exothermic and enthalpy-driven.

- The configuration located at  $Z = 6.5 \text{ \AA}$  for B mode represents the most stable configuration with a complexation energy of  $-70.66 \text{ kJ/mol}$  as calculated with PBEh-3c in vacuum.

- The structural analysis showed that PCP penetrates partially the  $\beta$ -cyclodextrin cavity.

- Hydrogen bonding and Van der Waals interactions were found by IGMH analysis to be the main driving forces for the formation and stabilization of the PCP@ $\beta$ -CD complex.

- Upon complexation, a significant hydrogen bond was formed at a short distance of  $1.62 \text{ \AA}$  with a stabilization energy of  $139.03 \text{ kJ/mol}$ .

- After complexation, the HOMO-LUMO energy gap decreased by a percentage of 30.58%, suggesting the potential application of the  $\beta$ -CD host system for the encapsulation of PCP.

The results of this study revealed the sensing potential of  $\beta$ -cyclodextrin as a suitable host in electronic devices based on biosensors for the detection, capture and encapsulation of pentachlorophenol. This work could serve as a starting point for more deep experimental studies for developing effective biosensors for environmental concerns.

## • Supplementary materials

No supplementary materials are available.

## • Funding

This research had no external funding.

## • Acknowledgments

None.

## • Author contributions

Conceptualization: Y.B, T.B.

Data curation: Z.K, R.L, A.M.

Formal Analysis: I.M.A, Z.K, A.L.

Funding acquisition: Y.B.

Investigation: R.L, A.M.

Methodology: Y.B., T.B.

Project administration: Y.B.

Resources: I.M.A., Z.K., A.L.

Software: Y.B., Z.K, A.L.

Supervision: Y.B., T.B.

Validation: Y.B.

Visualization: R.L., A.M., Z.K., A.L.

Writing – original draft: Y.B., I.M.A., Z.K.

Writing – review & editing: Y.B.

## • Conflict of interest

The authors declare no conflict of interest.

## • Additional information

Author ID:

Y. Belhocine, Scopus ID [54917426000](https://orcid.org/0000-0001-5491-7426).

Websites:

University of khenchela, <https://univ-khenchela.com>;

University of Skikda, <https://www.univ-skikda.dz/index.php/en>.

## References

1. Mattia E, Otto S. Supramolecular systems chemistry. Nat Nanotechnol. 2015;10:111-119. doi:[10.1038/nnano.2014.337](https://doi.org/10.1038/nnano.2014.337)
2. Kolesnichenko IV, Ansyn EV. Practical applications of supramolecular chemistry. Chem Soc Rev. 2017;46:2385-2390. doi:[10.1039/C7CS00078B](https://doi.org/10.1039/C7CS00078B)
3. Ma X, Zhao Y. Biomedical applications of supramolecular systems based on host-guest interactions. Chem Rev. 2014;115:7794-7839. doi:[10.1021/cr500392w](https://doi.org/10.1021/cr500392w)
4. Sambrook MR, Notman S. Supramolecular chemistry and chemical warfare agents: From fundamentals of recognition to catalysis and sensing. Chem Soc Rev. 2013;42:9251-9267. doi:[10.1039/C3CS60230C](https://doi.org/10.1039/C3CS60230C)
5. Bohmer V. Calixarenes, Macrocycles with (Almost) Unlimited Possibilities. Angew Chem Int Ed Engl. 1995;34:713-725. doi:[10.1002/anie.199507131](https://doi.org/10.1002/anie.199507131)
6. Chen JF, Ding JD, Wei TB. Pillararenes: Fascinating planar chiral macrocyclic arenes. Chem Commun. 2021;57:9029-9039. doi:[10.1039/D1CC03778A](https://doi.org/10.1039/D1CC03778A)
7. Gerasko OA, Samsonenko DG, Fedin VP. Supramolecular chemistry of cucurbiturils. Russ Chem Rev. 2002;71:741-760. doi:[10.1070/RC2002v071n09ABEH000748](https://doi.org/10.1070/RC2002v071n09ABEH000748)
8. Crini G. Review: a history of cyclodextrins. Chem Rev. 2014;114:10940-10975. doi:[10.1021/cr500081p](https://doi.org/10.1021/cr500081p)
9. Del Valle EM. Cyclodextrins and their uses: a review. Process Biochem. 2004;39(9):1033-1046. doi:[10.1016/S0032-9592\(03\)00258-9](https://doi.org/10.1016/S0032-9592(03)00258-9)

10. Crini G, Fourmentin S, Fenyvesi É, Torri G, Fourmentin M, Morin-Crini N. Cyclodextrins from molecules to applications. *Environ Chem Lett.* 2018;16:1361–1375. doi:[10.1007/s10311-018-0763-2](https://doi.org/10.1007/s10311-018-0763-2)
11. Gidwani B, Vyas A. Pharmacokinetic study of solid-lipid-nanoparticles of altretamine complexed epichlorohydrin- $\beta$ -cyclodextrin for enhanced solubility and oral bioavailability. *Int J Biol Macromol.* 2017;101:24–31. doi:[10.1016/j.ijbiomac.2017.03.047](https://doi.org/10.1016/j.ijbiomac.2017.03.047)
12. Alizadeh N, Malakzadeh S. Changes in chemical stability and bioactivities of curcumin by forming inclusion complexes of beta- and Gama-cyclodextrins. *J Polym Res.* 2020;27:42. doi:[10.1007/s10965-019-1994-z](https://doi.org/10.1007/s10965-019-1994-z)
13. Yadav M, Thakore S, Jadeja R. A review on remediation technologies using functionalized Cyclodextrin. *Environ Sci Pollut Res.* 2022;29:236–250. doi:[10.1007/s11356-021-15887-y](https://doi.org/10.1007/s11356-021-15887-y)
14. Roy I, Stoddart JF. Cyclodextrin metal-organic frameworks and their applications. *Acc Chem Res.* 2021;54(6):1440–1453. doi:[10.1021/acs.accounts.0c00695](https://doi.org/10.1021/acs.accounts.0c00695)
15. Liu Y, Lin T, Cheng C, Wang Q, Lin S, Liu C, Han X. Research progress on synthesis and application of cyclodextrin polymers. *Molec.* 2021;26(4):1090. doi:[10.3390/molecules26041090](https://doi.org/10.3390/molecules26041090)
16. Bautista-Renedo JM, Hernández-Esparza R, Cuevas-Yañez E, Reyes-Pérez H, Vargas R, Garza J, González-Rivas N. Deformations of cyclodextrins and their influence to form inclusion compounds. *Int J Quantum Chem.* 2021;122(6):e26859. doi:[10.1002/qua.26859](https://doi.org/10.1002/qua.26859)
17. Tian B, Hua S, Tian Y, Liu J. Cyclodextrin-based adsorbents for the removal of pollutants from wastewater: a review. *Environ Sci Pollut Res.* 2021;28:1317–1340. doi:[10.1007/s11356-020-11168-z](https://doi.org/10.1007/s11356-020-11168-z)
18. Majd M, Yazdanpanah M, Bayatloo MR, Nojavan S. Recent advances and applications of cyclodextrins in magnetic solid phase extraction. *Talanta.* 2021;229:122296. doi:[10.1016/j.talanta.2021.122296](https://doi.org/10.1016/j.talanta.2021.122296)
19. Nelumdeniya NRM, Ranatunga RJKU. Complex forming behaviour of  $\alpha$ ,  $\beta$  and  $\gamma$ -cyclodextrins with varying size probe particles in silico. *Ceylon J Sci.* 2021;50(5):329–339. doi:[10.4038/cjs.v50i5.7922](https://doi.org/10.4038/cjs.v50i5.7922)
20. United States Environmental Protection Agency. Pentachlorophenol. Available from: <https://www.epa.gov/ingredients-used-pesticide-products/pentachlorophenol>, Accessed on 03 August 2022.
21. United States Environmental Protection Agency. Priority Pollutant List, 2014. Available from: <https://www.epa.gov/sites/default/files/2015-09/documents/priority-pollutant-list-epa.pdf>, Accessed on 03 August 2022.
22. Agency for Toxic Substances and Disease Registry (ATSDR), 2001. Toxicological Profile for Pentachlorophenol Atlanta, GA: U.S. Available from: <https://semsub.epa.gov/work/10/100006534.pdf>, Accessed on 03 August 2022.
23. Kraševc I, Nemeček N, Lozar Štamcar M, Kralj Cigić I, Prosen H. Non-destructive detection of pentachlorophenol residues in historical wooden objects. *Polymers.* 2021;13(7):1052. doi:[10.3390/polym13071052](https://doi.org/10.3390/polym13071052)
24. Jambhekar SS, Breen P. Cyclodextrins in pharmaceutical formulations I: structure and physicochemical properties, formation of complexes, and types of complex. *Drug Discov Today.* 2016;21:356–362. doi:[10.1016/j.drudis.2015.11.017](https://doi.org/10.1016/j.drudis.2015.11.017)
25. Iacovino R, Rapuano F, Caso JV, Russo A, Lavorgna M, Russo C, Isidori M, Russo L, Malgieri G, Isernia C.  $\beta$ -Cyclodextrin inclusion complex to improve physicochemical properties of piperidic acid: Characterization and bioactivity evaluation. *Int J Mol Sci.* 2013;14:13022–13041. doi:[10.3390/ijms140713022](https://doi.org/10.3390/ijms140713022)
26. Bakó I, Jicsinszky L. Semiempirical calculations on cyclodextrins. *J Incl Phenom Macrocycl Chem.* 1994;18:275–289. doi:[10.1007/BF00708734](https://doi.org/10.1007/BF00708734)
27. Bouhadiba A, Belhocine Y, Rahim M, Djilani I, Nouar L, Khatmi DE. Host-guest interaction between tyrosine and  $\beta$ -cyclodextrin: Molecular modeling and nuclear studies. *J Mol Liq.* 2017;233:358–363. doi:[10.1016/j.molliq.2017.03.029](https://doi.org/10.1016/j.molliq.2017.03.029)
28. Fifere A, Marangoci N, Maier SS, Coroaba A, Maftai D, Pintea M. Theoretical study on  $\beta$ -cyclodextrin inclusion complexes with propiconazole and protonated propiconazole. *Beilstein J Org Chem.* 2012;8:2191–2201. doi:[10.3762/bjoc.8.247](https://doi.org/10.3762/bjoc.8.247)
29. Mazurek AH, Szeleszczuk Ł. Current status of quantum chemical studies of cyclodextrin host-guest Complexes. *Molecules* 2022;27:3874. doi:[10.3390/molecules27123874](https://doi.org/10.3390/molecules27123874)
30. Mesri N, Belhocine Y, Messikh N, Sayede A, Mouffok B. Molecular DFT investigation on the inclusion complexation of Benzo[a]pyrene with  $\gamma$ -Cyclodextrin. *Macrocyclic Chem.* 2021;14(2):164–170. doi:[10.6060/mhc210337m](https://doi.org/10.6060/mhc210337m)
31. Oqmhula K, Hongo K, Maezono R, Ichihba T. Ab Initio evaluation of complexation energies for cyclodextrin-drug inclusion complexes. *ACS Omega* 2020;5:19371–19376. doi:[10.1021/acsomega.0c01059](https://doi.org/10.1021/acsomega.0c01059)
32. Hanna K, de Brauer C, Germain P. Cyclodextrin-enhanced solubilization of pentachlorophenol in water. *J Environ Manag.* 2004;71(1):1–8. doi:[10.1016/j.jenvman.2004.01.001](https://doi.org/10.1016/j.jenvman.2004.01.001)
33. Neese F. The ORCA program system. *Wiley Interdiscip. Rev. Comput Mol Sci.* 2012;2:73–78. doi:[10.1002/wcms.81](https://doi.org/10.1002/wcms.81)
34. Neese F. Software update: the ORCA program system, version 4.0. *WIREs. Comput Mol Sci.* 2017;8:e1327. doi:[10.1002/wcms.1327](https://doi.org/10.1002/wcms.1327)
35. Becke AD. Density-functional exchange-energy approximation with correct asymptotic behavior. *Phys Rev A.* 1988;38:3098–3100. doi:[10.1103/PhysRevA.38.3098](https://doi.org/10.1103/PhysRevA.38.3098)
36. Lee C, Yang W, Parr RG. Development of the Colle-Salvetti correlation-energy formula into a functional of the electron density. *Phys Rev B.* 1988;37:785–789. doi:[10.1103/PhysRevB.37.785](https://doi.org/10.1103/PhysRevB.37.785)
37. Caldeweyher E, Ehlert S, Hansen A, Neugebauer H, Spicher S, Bannwarth C, Grimme S. A generally applicable atomic-charge dependent London dispersion correction. *J Chem Phys.* 2019;150:154122. doi:[10.1063/1.5090222](https://doi.org/10.1063/1.5090222)
38. Belhocine Y, Rahali S, Allal H, Assaba IM, Ghoniem MG, Ali FAM. A dispersion corrected DFT investigation of the inclusion complexation of dexamethasone with  $\beta$ -Cyclodextrin and molecular docking study of its potential activity against COVID-19. *Molec.* 2021;26:7622. doi:[10.3390/molecules26247622](https://doi.org/10.3390/molecules26247622)
39. Litim A, Belhocine Y, Benlecheb T, Ghoniem MG, Kabouche Z, Ali FAM, Abdulkhair BY, Seydou M, Rahali S. DFT-D4 Insight into the Inclusion of Amphetamine and Methamphetamine in Cucurbit[7]uril: Energetic, Structural and Biosensing Properties. *Molec.* 2021;26:7479. doi:[10.3390/molecules26247479](https://doi.org/10.3390/molecules26247479)
40. Kruse H, Grimme S. A geometrical correction for the inter- and intra-molecular basis set superposition error in Hartree-Fock and density functional theory calculations for large systems. *J Chem Phys.* 2012;136:154101. doi:[10.1063/1.3700154](https://doi.org/10.1063/1.3700154)
41. Liu L, Guo QX. Use of quantum chemical methods to study cyclodextrin chemistry. *J Incl Phenom Macrocycl Chem.* 2004;50:95–103. doi:[10.1007/s10847-003-8847-3](https://doi.org/10.1007/s10847-003-8847-3)
42. Jmol: an open-source Java viewer for chemical structures in 3D. Available from: <http://www.jmol.org/>
43. Grimme S, Brandenburg JG, Bannwarth C, Hansen A. Consistent structures and interactions by density functional theory with small atomic orbital basis sets. *J Chem Phys.* 2015;143:054107. doi:[10.1063/1.4927476](https://doi.org/10.1063/1.4927476)
44. Marenich AV, Cramer CJ, Truhlar DG. Universal Solvation Model Based on Solute Electron Density and on a Continuum Model of the Solvent Defined by the Bulk Dielectric Constant and Atomic Surface Tensions. *J Phys Chem B* 2009;113(18):6378–6396. doi:[10.1021/jp810292n](https://doi.org/10.1021/jp810292n)
45. Lefebvre C, Khartabil H, Boisson JC, Contreras-García J, Piquemal JP, Hénon E. The Independent Gradient Model: A New Approach for Probing Strong and Weak Interactions in Molecules from Wave Function Calculations. *ChemPhysChem* 2018;19:724–735. doi:[10.1002/cphc.201701325](https://doi.org/10.1002/cphc.201701325)

46. Lu T, Chen Q. Independent gradient model based on Hirshfeld partition: A new method for visual study of interactions in chemical systems. *J Comput Chem.* 2022;43:539–555. doi:[10.1002/jcc.26812](https://doi.org/10.1002/jcc.26812)
47. Lu T, Chen F. Multiwfn: a multifunctional wavefunction analyzer. *J Comput Chem.* 2012;33:580–592. doi:[10.1002/jcc.22885](https://doi.org/10.1002/jcc.22885)
48. Humphrey W, Dalke A, Schulten K. VMD: visual molecular dynamics. *J Mol Graph.* 1996;14:33–38. doi:[10.1016/0263-7855\(96\)00018-5](https://doi.org/10.1016/0263-7855(96)00018-5)
49. Knizia G. Intrinsic atomic orbitals: An unbiased bridge between quantum theory and chemical concepts. *J Chem Theory Comput.* 2013;9(11):4834–4843. doi:[10.1021/ct400687b](https://doi.org/10.1021/ct400687b)
50. Knizia G, Klein JE. Electron flow in reaction mechanisms—Revealed from first principles. *Angew Chem Int Ed.* 2015;54(18):5518–5522. doi:[10.1002/anie.201410637](https://doi.org/10.1002/anie.201410637)
51. González GB, Espinoza JM. Thermodynamic and reactivity aspect of  $\beta$ -cyclodextrine inclusion complexes with coumarin derivatives. *J Chil Chem Soc.* 2022;67(2):5514–5520. doi:[10.4067/S0717-97072022000205514](https://doi.org/10.4067/S0717-97072022000205514)
52. Belhocine Y, Bouhadiba A, Rahim M, Nouar L, Djilani I, Khatmi DE. Inclusion complex formation of  $\beta$ -Cyclodextrin with the nonsteroidal anti-inflammatory drug flufenamic acid: computational study. *Macroheterocycles.* 2018;11(2):203–209. doi:[10.6060/mhc170829b](https://doi.org/10.6060/mhc170829b)
53. Reed AE, Curtiss LA, Weinhold F. Intermolecular interactions from a natural bond orbital, donor-acceptor viewpoint. *Chem Rev.* 1998;88:899–926. doi:[10.1021/cr00088a005](https://doi.org/10.1021/cr00088a005)
54. Zhao Y, Truhlar DG. The Mo6 suite of density functionals for main group thermochemistry, thermochemical kinetics, non-covalent interactions, excited states, and transition elements: two new functionals and systematic testing of four Mo6-class functionals and 12 other functionals. *Theor Chem Account.* 2008;120:215–241. doi:[10.1007/s00214-007-0310-x](https://doi.org/10.1007/s00214-007-0310-x)
55. Weigend F. Accurate Coulomb-fitting basis sets for H to Rn. *Phys Chem Chem Phys.* 2006;8:1057–1065. doi:[10.1039/B515623H](https://doi.org/10.1039/B515623H)
56. Weigend F, Ahlrichs R. Balanced basis sets of split valence, triple zeta valence and quadruple zeta valence quality for H to Rn: Design and assessment of accuracy. *Phys Chem Chem Phys.* 2005;7:3297–3305. doi:[10.1039/B508541A](https://doi.org/10.1039/B508541A)
57. Frisch MJ, Trucks GW, Schlegel HB, Scuseria GE, Robb MA, Cheeseman JR, et al. Gaussian 09, Revision D.01, Gaussian Inc., Wallingford (CT), 2013.